Oscillations Make Neural Networks Robust to Quantization

Anonymous authors
Paper under double-blind review

Abstract

We challenge the prevailing view that weight oscillations observed during Quantization Aware Training (QAT) are merely undesirable side-effects and argue instead that they are an essential part of QAT. We show in a linear model with a single weight that the straight-through estimator (STE) results in an additional loss term that causes oscillations by pushing weights towards the *nearest quantization levels*. Based on the mechanism from the analysis, we then derive a regularizer that induces oscillations in the weights of neural networks during training. Our empirical results on ResNet-18 and Tiny ViT on CIFAR-10 and Tiny ImageNet datasets demonstrate across a range of quantization levels that training with oscillations followed by post-training quantization (PTQ) is sufficient to recover the performance of QAT in most cases. With this work we shed further light on the dynamics of QAT and contribute a novel insight into explaining the role of oscillations in QAT which until now have been considered to have a primarily negative effect on quantization.

1 Introduction

Deep neural networks have grown increasingly powerful at many tasks, but also increasingly expensive to use. As model sizes balloon into the hundreds of millions of parameters, the cost of inference has become a significant bottleneck, particularly for deployment on edge devices or usage in large-scale services (Sevilla et al., 2022). To reduce this cost, quantization of model weights has emerged as a prominent strategy (Nagel et al., 2021).

But weight quantization comes with its own cost, namely, drop in accuracy. Reducing precision introduces quantization error, and naive approaches like Post-Training Quantization (PTQ) often lead to sharp degradations in model performance at low bit widths. To combat this degradation in accuracy, many methods have been proposed, usually centered around minimizing the quantization error (Hung et al., 2015; Hirose et al., 2017; Li et al., 2020; Choi et al., 2020; Han et al., 2021; Zhong et al., 2025).

Yet these approaches fall short of Quantization-Aware Training (QAT) (Jacob et al., 2018; Krishnamoorthi, 2018), which simply incorporates quantization into the training loop, resulting in models that are robust to quantization. Unfortunately, QAT brings its own mysteries. Despite its empirical success, the underlying behavior of QAT remains poorly understood. In particular, QAT often exhibits a seemingly strange phenomenon: *oscillations* in the weights. Rather than settling into a stable state, quantized weights fluctuate between adjacent quantization levels. These oscillations are widely seen as *undesirable artifacts* introduced by the Straight-Through Estimator (STE). Several works have tried to suppress these weight oscillations mainly through dampening or weight freezing (Défossez et al., 2021; Nagel et al., 2022; Huang et al., 2023; Gupta & Asthana, 2024; Liu et al., 2023).

This paper poses the question: *What if we had this view on oscillations in QAT backwards?* To the best of our knowledge, we are the first to argue that the phenomenon of weight oscillations in QAT is not a bug, but a feature. Using a toy model, we show that oscillations arise from a gradient component in QAT which pushes weights towards the nearest quantization threshold – this stands in contrast to aligning weights at the quantization level, which would minimize the quantization error. We then induce such oscillations to push the weights towards the nearest thresholds deliberately during the model training. This is realized as a simple regularization term that pushes weights towards their nearest quantization threshold. Surprisingly, this

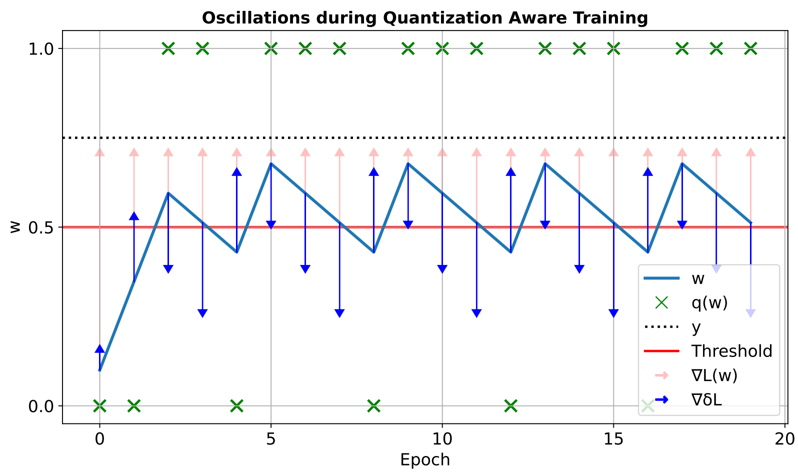

Figure 1: Oscillatory behavior during QAT in a one weight linear model $\hat{y} = q(w)x$, with input $x = 1$ and target $y = 0.75$. The gradient of this model during QAT can be decomposed into two terms: $\nabla L(w)$ and $\nabla \delta_L = q(w) - w$, where the latter term is what differentiates QAT from just optimizing the full precision loss $L(w)$. During QAT, $\nabla L(w)$ always points towards y, while $\nabla \delta_L$ introduces a dynamic which pushes w towards the nearest bin threshold. This causes w to oscillate when y is not exactly on a quantization level. In the above case this makes $q(w)$ alternate between 0 and 1. Note the frequency of oscillations of $q(w)$ lets the quantized weight on average to converge to 0.75.

leads to models that are robust to quantization and in most cases we find that these regularization-induced oscillations recover the accuracy obtained with QAT. Additionally, in many cases, oscillations outperform QAT under cross-bit evaluation (i.e. testing at precision levels not simulated during training). These findings further deepen our understanding of QAT and point to a more nuanced role for weight oscillations; suggesting they may be beneficial to QAT rather than being solely detrimental as argued in most existing literature.

Our primary contributions supporting this claim are:

1. Using a toy model we illustrate how the Straight Through Estimator (STE) leads to oscillations and clustering of model weights during QAT (Sec. 3);
2. We show experimentally that by using a mechanism inspired by the toy model, we can induce oscillations and clustering during training in neural networks (Sec. 4).
3. We empirically confirm using the CIFAR-10 (Krizhevsky et al., 2009) and Tiny-ImageNet (Le & Yang, 2015) datasets on a multi-layer perceptron (MLP), ResNet-18 (He et al., 2016) and Tiny Vision transformer (Tiny ViT) (Wu et al., 2022) that introducing oscillations through regularization in most cases recovers the accuracy of QAT (Sec. 5).

2 Preliminaries and Related Work

Quantization: A quantizer divides a continuous input range into quantization bins, where each bin is represented by a specific quantization level. The boundaries between bins are called quantization thresholds. During quantization, any value within a bin is mapped to that bin's quantization level. With a uniform quantizer, the step size (the distance between two adjacent quantization levels) is equal to the scale factor s.

We consider a uniform symmetric quantizer with a max-range scale factor. The quantization operation $q(\cdot)$ can then be expressed as

$$q(\mathbf{w}) = s \cdot \left\lceil \frac{\mathbf{w}}{s} \right\rfloor \quad (1)$$

Here, s represents the scale factor and $\lceil\cdot\rfloor$ denotes the rounding operation.

The scale factor s is set to cover the range of $\mathbf{w}$ as this removes the need for the usual clamping operation in the quantizer, while keeping the number of bins symmetric around 0:

$$s = \frac{\max(|\alpha|, |\beta|)}{2^{b-1} - 1} \tag{2}$$

where b is the bit in the quantizer and α, β are the minimum and maximum values, respectively, of the layer wise weights $\mathbf{w}$.

The quantization process introduces quantization error $\mathbf{\Delta}$, defined as the difference between the original and quantized values:

$$\mathbf{\Delta}(\mathbf{w}) = \mathbf{w} - q(\mathbf{w}) \tag{3}$$

Due to the uniform quantizer, for all bins the absolute error is bounded between $0 \leq |\mathbf{\Delta}| \leq s/2$, which is maximized at quantization thresholds and 0 at quantization levels.

Quantization-Aware Training: While there exist many variants of QAT, fundamentally the forward pass is performed using the quantized weights $q(\mathbf{w})$ in most variants of QAT (Jacob et al., 2018; Krishnamoorthi, 2018), simulating the effect of using low-precision weights. In principle the gradient for the weights during QAT is given by:

$$\frac{\partial \mathcal{L}(q(\mathbf{w}))}{\partial \mathbf{w}} = \frac{\partial \mathcal{L}(q(\mathbf{w}))}{\partial q(\mathbf{w})} \cdot \frac{\partial q(\mathbf{w})}{\partial \mathbf{w}} \tag{4}$$

A problem with the above formulation is that the gradient of the rounding operation used in the quantizer is zero almost everywhere, causing the last term to interrupt gradient-based learning. A popular solution to this problem is to use the so-called Straight-Through Estimator (STE) (Bengio et al., 2013). We define the STE to be the operator $\frac{\hat{\partial}}{\partial \mathbf{x}}$ such that $\frac{\hat{\partial} f}{\partial x}$ is obtained by computing $\frac{\partial f}{\partial x}$ and in the resulting expression replacing q' (the derivative of q) by the constant function equal to 1. In other words, if $\frac{\partial f}{\partial x} = g(\ldots, q', \ldots)$ then $\frac{\hat{\partial} f}{\partial x} = g(\ldots, 1, \ldots)$.

Related Work: Minimizing the quantization error is the most commonly used strategy to reduce the impact of quantization on model accuracy. This can be achieved by adjusting the granularity of the quantizer – for instance, using per-channel (Nagel et al., 2019) or block-wise quantization (Dettmers et al., 2022) instead of per-tensor quantization. While these methods reduce quantization error without additional training, they come with increased storage requirements due to extra quantization parameters and may still fall short at low bit widths, necessitating the combination with other approaches.

Consequently, extensive research has been dedicated to developing techniques that explicitly minimize the quantization error during optimization (Hung et al., 2015; Hirose et al., 2017; Li et al., 2020; Choi et al., 2020; Han et al., 2021; Zhong et al., 2025).

Despite these efforts, the aforementioned strategies often fall short of the accuracy obtained with QAT (Jacob et al., 2018) at individual bits or indirectly rely upon QAT themselves. In short, QAT integrates the quantization process into the training loop allowing the model to adapt to the quantization effects directly. This is done by quantizing the weights during the forward pass and using techniques like STE to approximate the gradient of the quantizer (which has a derivative of zero almost everywhere) during backpropagation (Bengio et al., 2013).

There is limited understanding of how QAT affects model optimization and why it outperforms other methods. One phenomenon observed during QAT is weight oscillations (Défossez et al., 2021; Nagel et al., 2022), which are periodic changes in the value of the quantized weight between two adjacent quantization levels. It is speculated in these works that the abrupt changes in values caused by oscillations can interfere negatively with optimization. Oscillations are assumed to be undesirable side effects caused by the use of the STE during backpropagation, as the STE allows gradients to pass through the rounding operation in the quantizer, which has a gradient of zero almost everywhere (Défossez et al., 2021; Nagel et al., 2022).

Several approaches have been suggested to mitigate oscillations by either freezing or dampening (Défossez et al., 2021; Nagel et al., 2022; Huang et al., 2023; Gupta & Asthana, 2024; Liu et al., 2023). However, the reported accuracy gains are sometimes marginal, and these methods may inadvertently also hinder the optimization process. For instance, Nagel et al. (2022) notes that freezing or dampening weights too early during training can hurt optimization, indicating that oscillations might contribute to finding better quantized minima of the loss. Liu et al. (2023) propose that weights with low oscillation frequency should be frozen, where as high-frequency ones should be left unfrozen, under the rationale that high frequency means the network has little confidence in what value to quantize the weight to, whereas low frequency means the optimal weight lies close to a quantization level.

3 Oscillations in QAT

Previous studies have explored linear models to analyze the behavior of QAT and the phenomenon of weight oscillations (Défossez et al., 2021; Nagel et al., 2022; Liu et al., 2023; Gupta & Asthana, 2024). Inspired by these works, we also analyze a linear regression model to gain insights into the optimization dynamics during QAT.

3.1 Toy Model

Consider a linear model with a single weight w, input x and target $y \in \mathbb{R}$. The quantized version of this model is defined as $\hat{y} = q(w)x$, where $q(\cdot)$ is the quantizer from Eq. 1. The quadratic loss for the quantized model is given by

$$\mathcal{L}(q(w)) = \frac{1}{2}(\hat{y} - y)^2 = \frac{1}{2}(q(w)x - y)^2. \tag{5}$$

Our goal in this section is to understand how QAT affects the full precision optimization process. For a given loss function $\mathcal{L}(\cdot)$ with quantized weights, we have

$$\mathcal{L}(q(w)) = \mathcal{L}(w) + \mathcal{L}(q(w)) - \mathcal{L}(w) \tag{6}$$

We can then expand the difference in loss caused by quantization as follows:

$$\delta_{\mathcal{L}} = \mathcal{L}(q(w)) - \mathcal{L}(w) = \frac{1}{2}\left((q(w)x - y)^2 - (wx - y)^2\right) \tag{7}$$

$$= \frac{1}{2}\left(x^2\left(q(w)^2 - w^2\right)\right) + (yx(w - q(w))) \tag{8}$$

This expression decomposes the loss difference $\delta_{\mathcal{L}}$ into a quadratic term $\frac{1}{2}x^2(q(w)^2 - w^2)$ and a linear term $yx(w - q(w))$.

Next we derive the gradient of $\delta_{\mathcal{L}}$ wrt. w:

$$\frac{\partial \delta_{\mathcal{L}}}{\partial w} = \frac{\partial}{\partial w}\Big(\mathcal{L}(q(w)) - \mathcal{L}(w)\Big) = \frac{\partial}{\partial w}\left(\frac{1}{2}x^2(q(w)^2 - w^2) + yx(w - q(w))\right) \tag{9}$$

$$= x^2\left(q(w)\frac{\partial q(w)}{\partial w} - w\right) + yx\left(1 - \frac{\partial q(w)}{\partial w}\right) \tag{10}$$

Using the STE and recalling that $\frac{\hat{\partial} q}{\hat{\partial} w} = 1$ the expression of the STE gradient simplifies to[1]

$$\frac{\hat{\partial}\delta_{\mathcal{L}}}{\hat{\partial} w} = x^2(q(w) - w) = -x^2\mathbf{\Delta}(w). \tag{11}$$

[1] Note that there is no clamping in the quantizer because of the scale factor Eq. (2).

3.2 Oscillation Mechanism

To see how the observations in Sec. 3.1 gives rise to oscillations, for an arbitrary w, denote w_0 the upper quantization threshold $w_0 = q(w)+s/2$. For $\varepsilon \in (0, s/2)$ note that we have $q(w_0-\varepsilon) = q(w)$ and $q(w_0+\varepsilon) = q(w)+s$ so that

$$\mathbf{\Delta}(w_0+\varepsilon) = q(w)+s/2+\varepsilon-(q(w)+s) = -s/2+\varepsilon, \tag{12}$$

$$\mathbf{\Delta}(w_0-\varepsilon) = q(w)+s/2-\varepsilon-q(w) = s/2-\varepsilon. \tag{13}$$

Assuming $x \neq 0$, the negative STE gradient "flips" from $-s/2$ to $+s/2$ as the weight w passes the quantization threshold w_0 from above, pushing the weight back towards the threshold. We note that the STE gradient is 0 at the special value $w = q(w)$, but the preceding argument shows that this is an unstable critical point and gradient noise will immediately cause the weights to move away from it. When combined with (stochastic) gradient descent and a finite discretization timestep we can identify this as the driving mechanism behind oscillations during training with QAT (Fig. 1).

3.3 Weight Clustering

We can also see how the dynamics described above can lead to weight clustering around quantization thresholds by looking at the sign of $\mathbf{\Delta}$ for different values of w. For a weight w let $d_{\text{low}}(w)$ and $d_{\text{up}}(w)$ denote the distance from w to the upper and lower thresholds, $d_{\text{low}}(w) = w - \left(q(w) - \frac{s}{2}\right) = \mathbf{\Delta}(w) + \frac{s}{2}$ and $d_{\text{up}}(w) = \left(q(w) + \frac{s}{2}\right) - w = \frac{s}{2} - \mathbf{\Delta}(w)$ respectively. If w is closest to the upper threshold we have

$$d_{\text{up}} < d_{\text{low}} \implies \tfrac{s}{2} - \mathbf{\Delta} < \mathbf{\Delta} + \tfrac{s}{2} \implies \mathbf{\Delta} > 0 \tag{14}$$

While if w is closest to the lower threshold

$$d_{\text{low}} < d_{\text{up}} \implies \mathbf{\Delta} + \tfrac{s}{2} < \tfrac{s}{2} - \mathbf{\Delta} \implies \mathbf{\Delta} < 0 \tag{15}$$

We emphasize that this mechanism causes the weight to move towards the quantization thresholds (the edges of quantization "bins") as opposed to the quantization levels (the centers of the quantization "bins"). As we saw above, the magnitude of the pull towards the threshold increases as the weight approach the threshold, so that the weight eventually crosses the threshold and ends up oscillating, unless $L(w)$ and δ_L exactly cancel out, which is unlikely to happen with a finite step size of gradient descent.

4 Regularization Method

Our theoretical observations in the linear model in Sec. 3, show that the oscillation component is the only part that differentiates QAT from normal, full precision, training. We now confirm empirically that the mechanism in Eq. (11) is sufficient to introduce weight oscillations during training of neural networks, and study if this also results in QAT-like behaviour with respect to the quantization noise.

From the quantization difference in Eq. 8 and the STE gradient derived in Eq. 11, we have:

$$\frac{\partial \mathcal{L}(q(w))}{\partial w} = \frac{\partial \mathcal{L}(w)}{\partial w} - x^2 \mathbf{\Delta}(w) \tag{16}$$

where the first term is the gradient of the original full-precision loss, and the second term causes the quantization oscillations in QAT.

In order to emulate the effects described in Section 3, we propose a regularization term so that the training objective becomes:

$$\mathcal{L}(\mathbf{w}) + \mathcal{R}_\lambda(\mathbf{w}) \tag{17}$$

where we let the regularization term be similar to the quadratic term in Eq. (8):

$$\mathcal{R}_\lambda(\mathbf{w}) = \frac{\lambda}{2} \sum_\ell \frac{1}{n_\ell} \sum_{i=1}^{n_\ell} \left(q(w_i^\ell)^2 - (w_i^\ell)^2 \right). \tag{18}$$

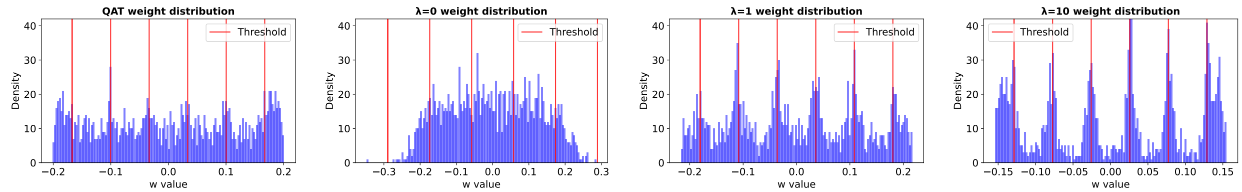

(a) (b) (c) (d)

Figure 2: Weight distribution analysis of ResNet-18's first convolutional layer after 50 epochs of training from scratch. a) Weight distribution under QAT with a 3-bit quantizer. b)-d) Our proposed regularization approach with a 3-bit quantizer at varying regularization strengths ($\lambda = 0, 1, 10$, from left to right). When $\lambda = 0$, the training reduces to standard optimization. The QAT distribution (leftmost) exhibits the characteristic threshold clustering behavior. As λ increases, we observe progressively stronger clustering of weights around quantization thresholds, illustrating the relationship between regularization strength and weight clustering.

.

Here $\lambda \geq 0$ is a hyperparameter that controls the amount of regularization, ℓ ranges over the layers in the model and i over the weights in each layer. In this term, we replaced the factor x^2 by a hyperparameter λ, since the precise expression of x^2 is specific to the model studied in Sec. 3. We empirically find that this regularizer is sufficient to induce oscillations. The exploration of the design space of oscillation-inducing regularizers, including layer-dependent and/or adaptive scale factors, is left to future work.

Using the STE, $\frac{\hat{\partial} q}{\partial \mathbf{w}} = 1$, we have the following expression for the gradient:

$$\frac{\hat{\partial}}{\hat{\partial} w_i^\ell} \mathcal{R}_\lambda(\mathbf{w}) = \frac{\lambda}{n_\ell} \left(q(w_i^\ell) - w_i^\ell \right) = -\frac{\lambda}{n_\ell} \mathbf{\Delta}(w_i^\ell). \tag{19}$$

By the same reasoning as in Sec. 3 this pulls the weight w_i^ℓ towards the quantization threshold and causes the gradient to "flip" as w_i^ℓ crosses the threshold. We expect this to lead to oscillations based on the same mechanism as in the model from Sec. 3.

Figures 2 and 3 show the results of an experiment where we observe the weight distributions, and measured the oscillations, during training of a neural network (ResNet-18) with varying degrees of regularization, respectively. For comparison purposes the figures also show the weight distributions and oscillations observed during training with QAT. Using the definition of an oscillation established in Nagel et al. (2022), we count an oscillation at epoch $i > 1$ if $q(w_t) \neq q(w_{t-1})$ and the direction of the change in the quantized space is opposite to that of the previous change.

Our first observation is that QAT displays more oscillations Fig. 2-a) than a baseline model without QAT or regularization (corresponding to $\lambda = 0$ in Fig. 3-b)). As we increase λ we observe that the number of oscillations as well as the clustering increases. This confirms that the regularizer from Eq. 18 can indeed induce oscillations similar to QAT during the training of deep neural networks. At $\lambda = 1$ (Fig. 3-c)) the number of oscillations observed with regularization is similar to the behaviour of QAT, lending support to our hypothesis that the mechanism in (12) is indeed at the root of the oscillations observed when training neural networks with QAT.

5 Experiments & Results

In this section, using empirical evidence we empirically answer the question: *Is it sufficient to induce weight oscillations during training in order to get the benefits of QAT?*

We answer this question affirmatively based on the results of training ResNet-18 and Tiny ViT on the CIFAR-10 and Tiny-ImageNet datasets. This is both in the training-from-scratch setting and when fine-tuning pretrained models.

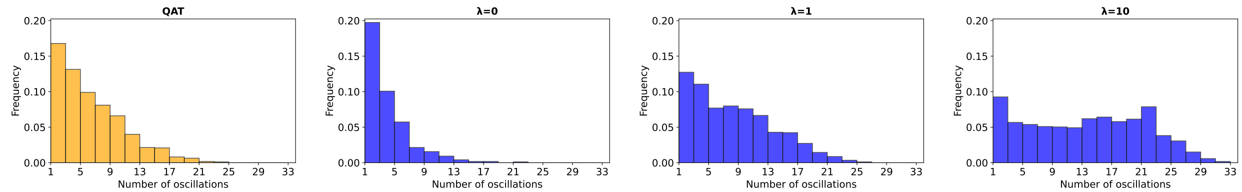

(a) (b) (c) (d)

Figure 3: Distribution of weight oscillations. The plots show the distribution of weights with oscillation counts > 0 when training with a) QAT and b)-d) the regularizer for different values of λ. Here $\lambda = 0$ corresponds to a full precision model where the regularizer has no influence on training. The y-axis represents the percentage of total weights in the first convolutional layer of a ResNet-18 trained from scratch for 50 epochs, while the x-axis shows the oscillation count. Following the oscillation definition from (Nagel et al., 2022), we count oscillations at each epoch during training. The results demonstrate that QAT produces a significantly higher proportion of oscillating weights compared to $\lambda = 0$. Furthermore, we observe that as we increase λ a greater percentage of weights oscillates.

In the following subsections we first describe the experimental setup, then we present the accuracy results from training-from-scratch and fine-tuning models trained with different quantization levels for the quantizer in $\mathcal{R}_\lambda$ or QAT and finally, we present the cross-bit accuracy of the fine-tuned models. We train models at ternary (3 possible values: -1, 0, 1), 3-bit and 4-bit. This is in line with contemporary research, where the emphasis lies on quantization at 4-bit and below since the challenges of maintaining accuracy are more significant compared to quantization at higher bit widths.

5.1 Experimental setup

We conducted our experiments using the CIFAR-10 (Krizhevsky et al., 2009) and Tiny-ImageNet (Le & Yang, 2015) datasets. We evaluated three architectures; A multi-layer perceptron with 5 hidden layers and 256 neurons per layer (MLP5), ResNet-18 (He et al., 2016) and Tiny Vision transformer (Tiny ViT) (Wu et al., 2022).

For each architecture we used the Adam optimizer (Kingma, 2014) and tested multiple configurations: A baseline model to establish optimal floating-point accuracy and PTQ performance, a model with QAT and a model with regularization using Eq. 18. The two latter configurations are trained using 3-bit and 4-bit quantizers. In all our experiments we use the regularizer $\mathcal{R}_\lambda$ defined in Eq. (18) to induce oscillations (Marked as "Oscillations" in the result table).

Training from Scratch: For the MLP5 architecture, we used a learning rate of 10^{-3} and regularization parameter λ=1. The ResNet-18 was trained with a learning rate of 10^{-3} and λ=0.75 (see Appx. A.2 for our hyperparameter selection). We modified the ResNet-18 architecture by replacing the input layer with a smaller 3×3 kernel and adapting the final layer for 10-class classification of both ResNet-18 and Tiny ViT. Training proceeded for a maximum of 100 epochs with early stopping triggered after 10 epochs without improvement in validation performance. For quantized models, we monitored the quantized validation accuracy at the target bit precision, while for the baseline, we tracked floating-point accuracy.

Fine-tuning: We fine-tuned two ImageNet-1k (Deng et al., 2009) pre-trained models on CIFAR-10 and Tiny-ImageNet: a Tiny ViT (learning rate: 10^{-4}, λ=1, 0.75, 0.5 depending on bit) and a ResNet-18 (learning rate: 10^{-3}, λ=1, 0.75, 0.5 depending on bit). To maintain compatibility with the pre-trained architectures, we up-sampled both CIFAR-10 and Tiny-Imagenet images to 224×224 pixels. The λ parameter selection process for Tiny ViT is detailed in Appendix A.2. Fine-tuning continued for up to 200 epochs on CIFAR-10 and 50 epochs for Tiny-ImageNet, with early stopping after 30 epochs without improvement, using the same accuracy metrics as training from scratch.

Quantization: We implemented weight quantization using a per-tensor uniform symmetric quantizer as defined in Eq. 1. PTQ is applied in its most minimal form, by simply quantizing the weights without any calibration. QAT is used as defined in Eq.4. The quantization range was determined by computing min-

Quantization	MLP5 (FS)	ResNet-18 (FS)	Tiny ViT (FT)	ResNet-18 (FT)
Baseline FP32	51.43 ± 0.39	83.26 ± 1.07	96.11 ± 0.31	88.50 ± 0.64
3-bit PTQ	20.97 ± 5.64	77.79 ± 4.00	11.56 ± 1.99	10.28 ± 0.48
3-bit QAT	50.53 ± 1.43	82.51 ± 2.14	88.13 ± 0.60	85.69 ± 1.83
3-bit Oscillations	48.48 ± 0.29	81.77 ± 0.46	88.68 ± 1.08	84.94 ± 1.59
4-bit PTQ	46.50 ± 0.76	82.11 ± 1.21	21.57 ± 5.33	35.56 ± 9.05
4-bit QAT	51.39 ± 0.60	82.66 ± 2.57	94.96 ± 0.33	87.71 ± 1.14
4-bit Oscillations	50.72 ± 0.47	83.74 ± 0.59	94.82 ± 0.51	87.08 ± 0.72

Table 1: Performance comparison on CIFAR-10 dataset. Results show classification accuracy for MLP5, ResNet-18, and Tiny ViT across different quantization approaches and bit-widths. Models trained from scratch are marked FS, and fine-tuning experiments are marked FT. FT experiments are based on models pre-trained on ImageNet-1k. In all cases oscillations followed by quantization of the weights matches QAT accuracy. Results are means and standard deviations over 5 random seeds. PTQ results are from the FP32 baseline.

imum and maximum values per layer. In our implementation of ResNet-18 (11M parameters) all layers except batch normalization were quantized, covering 99.96% of parameters. For Tiny ViT (5.5M parameters) quantization was applied to MLP, Self-Attention, and key-query-value projection layers, encompassing 97.18% of parameters. And lastly for the MLP5 model all layers were quantized. For Tiny-ImageNet models are trained at 3 and 4-bit precision only.

5.2 Results

The performance on the two datasets in training-from-scratch and fine-tuning settings is presented in the following sections, along with the observations about cross-bit generalization.

5.2.1 Performance on CIFAR-10

Training-from-scratch: Table 1 (A) shows the results from training an MLP and ResNet-18 from scratch on the CIFAR-10 dataset. Doing only regularization with Eq. 18 demonstrates improvements compared to the PTQ baseline. More importantly, it also matches the performance of QAT at bit widths of 3 and 4.

For both models we see that at 3-bit and 4-bit, using the $\mathcal{R}_\lambda$ regularizer from Eq. 18 exhibits similar performance as QAT but with less variability. With both models, QAT and $\mathcal{R}_\lambda$ regularization are competitive with the full-precision baseline. Notably, both $\mathcal{R}_\lambda$ regularization and QAT significantly outperform PTQ when applied to the full precision baseline.

Fine-tuning: Table 1 (B) summarizes the test accuracies for fine-tuning using our $\mathcal{R}_\lambda$ regularization and QAT on ResNet-18 and Tiny ViT architectures with CIFAR-10 and Tiny-ImageNet. The observations are roughly in line with the results observed for training from scratch in the previous section.

For CIFAR-10 as with the case for training from scratch, with both ResNet-18 and Tiny Vit we see an increase in performance compared to PTQ when using the regularization in Eq. 18. Regularization with $\mathcal{R}_\lambda$ and QAT show comparable performance when quantized at 3 bits and 4 bits, while achieving test accuracy close to the full precision model at 4-bits.

Performance comparison and related discussions for ternary quantization are presented in Appendix A.3.

Robustness to cross-bit quantization: In this experiment we evaluated the robustness of oscillations-only and QAT towards quantization at bit widths different from the ones used during training.

When using the $\mathcal{R}_\lambda$ regularization approach, we applied the regularization term with the training bit width during training and applied PTQ after training at a different quantization level. For QAT we trained using the training bit width and afterwards applied PTQ to the latent weights. For each method we also evaluated the corresponding model without PTQ, directly using the latent weights for inference (reported as FP32).

Model	Method ↓ / Eval. bit →	FP32	Tern.	3-bit	4-bit	8-bit
ResNet-18 (FT)	Baseline PTQ	88.50	10.01	10.28	35.56	88.45
	3-bit QAT	16.89	10.01	85.69	17.42	16.56
	3-bit Oscillations	**87.86**	**20.19**	84.94	**87.56**	**87.86**
	4-bit QAT	87.75	10.13	82.08	87.71	87.76
	4-bit Oscillations	87.85	11.91	85.57	87.08	87.87
Tiny ViT (FT)	Baseline PTQ	96.11	9.39	11.56	21.57	96.03
	3-bit QAT	86.94	**19.78**	88.13	86.69	86.95
	3-bit Oscillations	**96.47**	9.48	88.68	**95.35**	**96.50**
	4-bit QAT	95.14	11.11	59.86	94.96	95.13
	4-bit Oscillations	**96.54**	11.90	70.23	94.82	**96.55**

Table 2: Cross-bit evaluation of pre-trained ImageNet-1k models fine-tuned on CIFAR-10. Grey background is the target-bit accuracy. Models are trained using different quantization methods (QAT and ours) and bit-widths (ternary, 3-bit, and 4-bit), then evaluated across various bit-widths ranging from ternary to FP32. The grey diagonal shows the results for the bit used during training. Results are means and standard deviations over 5 random seeds. All significant differences between QAT and Oscillations are shown in bold face.

In Table 6 shows the results from the experiment. A first observation is that the models produced by $\mathcal{R}_\lambda$ regularization consistently achieve nearly full-precision accuracy when quantized at 8-bit or when used without quantization, irrespective of the quantization level used during training. This contrasts with QAT, which produces a viable 8-bit or full-precision model only when trained with at least 4-bit.

Furthermore we see that regularizing using Eq. 18 mostly maintains performance when trained at 3 or 4-bit and quantized at bit level of 3 or 4-bit. QAT also achieves this for Tiny ViT but for ResNet, the accuracy of QAT trained at 3-bit and quantized at other bit widths is barely above random guessing.

Regarding training with ternary quantization, we see that $\mathcal{R}_\lambda$ regularization produces models that achieve near full precision performance for ResNet when quantized at 3-bit or higher. Ternary training for ViT is somewhat peculiar in that it fails to produce a model that is viable when quantized to ternary, whereas the performance of the resulting models starts to show a high level of variability at 4-bit and finally reaches close to full-precision accuracy at 8-bit. In contrast, for both ResNet and ViT, the performance of QAT degrades completely to random guessing when trained with ternary quantization and evaluated at any other quantization level.

5.2.2 Performance on Tiny-ImageNet

Fine-tuning: Table 3 summarizes the test accuracies for the Tiny-ImageNet Dataset. Here we observe the same tendency as with CIFAR-10; oscillations provides a significant increase in accuracy compared to the PTQ baseline. While for the Tiny ViT model $\mathcal{R}_\lambda$ regularization is sufficient to recover the quantized accuracy of QAT in both the 3 and 4-bit case, for ResNet18 there is a degradation in accuracy at 3-bit.

Robustness to cross-bit quantization: In Table 4 we see the cross-bit results from the Tiny-ImageNet experiments. As with CIFAR-10 we note that the models produced by $\mathcal{R}_\lambda$ regularization achieves a better cross-bit performance at bits higher than the target bit. Though we do note a changes in the cross-bit behaviour; The cross-bit results for 3 and 4-bit is generally lower and not as close tot he FP baseline as in the CIFAR-10 case, yet still there is a significant difference between QAT and $\mathcal{R}_\lambda$ regularization.

6 Discussion

We have shown that training with weight oscillations induced via $\mathcal{R}_\lambda$ regularization is sufficient in most cases to maintain performance after quantization for ResNet and Tiny ViT. This begs the question whether weight oscillations are also a necessary part of the QAT training process. Indeed, some previous work already points towards this. There are examples claiming that both dampening and/or freezing of oscillations too early in

Quantization	Tiny ViT (FT)	ResNet-18 (FT)
Baseline FP32	67.17 ± 0.67	62.93 ± 0.55
3-bit PTQ	0.58 ± 0.16	0.51 ± 0.03
3-bit QAT	44.29 ± 0.49	54.08 ± 0.52
3-bit Oscillations	44.62 ± 2.47	49.34 ± 0.76
4-bit PTQ	11.02 ± 2.11	20.02 ± 4.80
4-bit QAT	60.61 ± 0.16	58.31 ± 0.19
4-bit Oscillations	60.54 ± 0.37	57.26 ± 0.33

Table 3: Accuracy on Tiny-ImageNet dataset. Mean and standard deviation is over 3 runs. The models is fine-tuned for 50 epochs on the pretrained ImageNet models. PTQ results is from the FP32 baseline. In both the 3 and 4 bit case, oscillations followed by quantization of the weights matches QAT and is noticeably above the PTQ baseline which has neither oscillations nor QAT.

Model	Method ↓ / Eval. bit →	FP32	Tern.	3-bit	4-bit	8-bit
ResNet-18 (FT)	Baseline PTQ	62.93	0.50	0.51	20.02	62.83
	3-bit QAT	50.81	4.51	54.08	49.76	50.85
	3-bit Oscillations	56.67	1.48	49.34	55.96	56.68
	4-bit QAT	56.57	0.65	39.65	58.31	56.66
	4-bit Oscillations	61.58	0.53	30.16	57.26	61.58
Tiny ViT (FT)	Baseline PTQ	67.17	0.49	0.58	11.02	67.06
	3-bit QAT	39.19	1.73	44.29	36.02	39.18
	3-bit Oscillations	56.75	1.51	44.62	56.22	56.78
	4-bit QAT	59.75	0.49	34.42	60.61	59.73
	4-bit Oscillations	65.58	0.54	22.26	60.54	65.60

Table 4: Cross-bit evaluation of pre-trained ImageNet-1k models fine-tuned on Tiny-ImageNet.

the training process is detrimental to performance after quantization (Nagel et al., 2022; Han et al., 2021). And in other case presented in Liu et al. (2023), freezing only the low frequency oscillating weights improves performance. This suggests that weight oscillations are both a necessary and sufficient part of QAT, at least in the early phases of the training process. This further supports our hypothesis that oscillations in QAT have a positive effect on quantization robustness overall.

Yet we do note deviations from QAT when regularizing with Eq. 18: QAT outperforms $\mathcal{R}_\lambda$ regularization at ternary quantization (Appendix A.3), whereas $\mathcal{R}_\lambda$ regularization outperforms QAT in cross-bit accuracy for the ternary and 3-bit case. In A.6, we see how it seems that the cross-bit performance for QAT is upper-bounded by the target-bit performance, which might explain the subpar QAT performance at cross-bit compared to $\mathcal{R}_\lambda$ regularization which seems bounded by the full precision accuracy.

Limitations and Future Work Our theoretical analysis was performed using the toy model in Section 3, and the regularization term is motivated using this analysis. We expect other effects that are not entirely captured by this analysis to be part of QAT. This is explored further in Appendix A.1, where we show how the second term is not zero in the gradient, when there are multiple layers.

The second term in Eq. 24 is closely related to the oscillations-dampening methods such as the one presented in Equation 6 in (Nagel et al., 2022). This shows that at least for the linear cases as analyzed in Appendix A.1, QAT consists solely of two components; one that creates oscillations and one that dampens them. In a way we can consider our work and (Nagel et al., 2022) as introducing *unstructured* oscillations and dampening, respectively. Whereas, in general, QAT could consists of more structured oscillations and dampening.

7 Conclusions

Based on the analysis of a linear model we hypothesized that weight oscillations during training in deep neural networks make the model robust to quantization akin to QAT. In Sections 3 and 4 we explain how training with QAT and STE leads to oscillations and propose a regularizer that encourages this oscillating behaviour. We confirm that as we increase the strength of the regularization, and empirically observe the appearance of clustering together with oscillations.

Finally, we experimentally confirm that the regularizer indeed leads to consistent robustness towards quantization for 3-bit and 4-bit quantization levels. Our oscillations by regularization approach achieves comparable performance to QAT above ternary quantization when quantizing to the target-bit seen during the optimization. Furthermore, we also observe that it shows increased robustness compared to QAT in cross-bit quantization with quantization levels higher than the target-bit used in the quantizer during training. All this being evidence of our hypothesis.

Our insights on weight oscillations and their role in quantization robustness open new horizons for model quantization approaches which usually build on the idea of aligning weights at quantization levels – the opposite of what seems to be the core dynamic in QAT. The regularization approach especially creates interesting possibilities for cross-bit robustness, potentially making the regularization method more appealing than QAT when the goal is to deploy or release a single set of model weights that can work across different bit widths or maybe even quantizers. While the regularizer used in our experiments should be viewed as an initial step, we expect that quantization robustness could be further improved by developing oscillation-inducing methods that are adaptive to different learning rates, layer statistics or phases of the training process.

Acknowledgments: Authors like to thank several people.

References

Yoshua Bengio, Nicholas Léonard, and Aaron Courville. Estimating or propagating gradients through stochastic neurons for conditional computation. *arXiv preprint arXiv:1308.3432*, 2013.

Yoojin Choi, Mostafa El-Khamy, and Jungwon Lee. Learning sparse low-precision neural networks with learnable regularization. *IEEE Access*, 8:96963–96974, 2020.

Alexandre Défossez, Yossi Adi, and Gabriel Synnaeve. Differentiable model compression via pseudo quantization noise. *arXiv preprint arXiv:2104.09987*, 2021.

Jia Deng, Wei Dong, Richard Socher, Li-Jia Li, Kai Li, and Li Fei-Fei. Imagenet: A large-scale hierarchical image database. In *2009 IEEE conference on computer vision and pattern recognition*, pp. 248–255. Ieee, 2009.

Tim Dettmers, Mike Lewis, Sam Shleifer, and Luke Zettlemoyer. 8-bit Optimizers via Block-wise Quantization. In *International Conference on Learning Representations*, 2022.

Kartik Gupta and Akshay Asthana. Reducing the side-effects of oscillations in training of quantized yolo networks. In *Proceedings of the IEEE/CVF Winter Conference on Applications of Computer Vision*, pp. 2452–2461, 2024.

Tiantian Han, Dong Li, Ji Liu, Lu Tian, and Yi Shan. Improving low-precision network quantization via bin regularization. In *Proceedings of the IEEE/CVF International Conference on Computer Vision*, pp. 5261–5270, 2021.

Kaiming He, Xiangyu Zhang, Shaoqing Ren, and Jian Sun. Deep residual learning for image recognition. In *Proceedings of the IEEE conference on computer vision and pattern recognition*, pp. 770–778, 2016.

Kazutoshi Hirose, Kota Ando, Kodai Ueyoshi, Masayuki Ikebe, Tetsuya Asai, Masato Motomura, and Shinya Takamaeda-Yamazaki. Quantization error-based regularization in neural networks. In *Artificial Intelligence XXXIV: 37th SGAI International Conference on Artificial Intelligence, AI 2017, Cambridge, UK, December 12-14, 2017, Proceedings 37*, pp. 137–142. Springer, 2017.

Xijie Huang, Zhiqiang Shen, Pingcheng Dong, and Kwang-Ting Cheng. Quantization variation: A new perspective on training transformers with low-bit precision. *arXiv preprint arXiv:2307.00331*, 2023.

Pei-Hen Hung, Chia-Han Lee, Shao-Wen Yang, V Srinivasa Somayazulu, Yen-Kuang Chen, and Shao-Yi Chien. Bridge deep learning to the physical world: An efficient method to quantize network. In *2015 IEEE Workshop on Signal Processing Systems (SiPS)*, pp. 1–6. IEEE, 2015.

Benoit Jacob, Skirmantas Kligys, Bo Chen, Menglong Zhu, Matthew Tang, Andrew Howard, Hartwig Adam, and Dmitry Kalenichenko. Quantization and training of neural networks for efficient integer-arithmetic-only inference. In *Proceedings of the IEEE conference on computer vision and pattern recognition*, pp. 2704–2713, 2018.

Diederik P Kingma. Adam: A method for stochastic optimization. *arXiv preprint arXiv:1412.6980*, 2014.

Raghuraman Krishnamoorthi. Quantizing deep convolutional networks for efficient inference: A whitepaper. *arXiv preprint arXiv:1806.08342*, 2018.

Alex Krizhevsky, Geoffrey Hinton, et al. Learning multiple layers of features from tiny images. 2009.

Ya Le and Xuan S. Yang. Tiny imagenet visual recognition challenge. 2015. URL https://api.semanticscholar.org/CorpusID:16664790.

Yuhang Li, Xin Dong, and Wei Wang. Additive powers-of-two quantization: An efficient non-uniform discretization for neural networks. In *International Conference on Learning Representations*, 2020. URL https://openreview.net/forum?id=BkgXT24tDS.

Shih-Yang Liu, Zechun Liu, and Kwang-Ting Cheng. Oscillation-free quantization for low-bit vision transformers. In *International Conference on Machine Learning*, pp. 21813–21824. PMLR, 2023.

Markus Nagel, Mart van Baalen, Tijmen Blankevoort, and Max Welling. Data-free quantization through weight equalization and bias correction. In *Proceedings of the IEEE/CVF International Conference on Computer Vision (ICCV)*, October 2019.

Markus Nagel, Marios Fournarakis, Rana Ali Amjad, Yelysei Bondarenko, Mart Van Baalen, and Tijmen Blankevoort. A white paper on neural network quantization. *arXiv preprint arXiv:2106.08295*, 2021.

Markus Nagel, Marios Fournarakis, Yelysei Bondarenko, and Tijmen Blankevoort. Overcoming oscillations in quantization-aware training. In *International Conference on Machine Learning*, pp. 16318–16330. PMLR, 2022.

Jaime Sevilla, Lennart Heim, Anson Ho, Tamay Besiroglu, Marius Hobbhahn, and Pablo Villalobos. Compute trends across three eras of machine learning. In *2022 International Joint Conference on Neural Networks (IJCNN)*, pp. 1–8. IEEE, 2022.

Kan Wu, Jinnian Zhang, Houwen Peng, Mengchen Liu, Bin Xiao, Jianlong Fu, and Lu Yuan. Tinyvit: Fast pretraining distillation for small vision transformers. In *European conference on computer vision*, pp. 68–85. Springer, 2022.

Yunshan Zhong, Yuyao Zhou, Fei Chao, and Rongrong Ji. Mbquant: A novel multi-branch topology method for arbitrary bit-width network quantization. *Pattern Recognition*, 158:111061, 2025.

A Appendix

A.1 2-layer with single weights

Consider a linear model $f(x) = w_2 w_1 x$, with w_1, w_2, input x, and target $y \in \mathbb{R}$. The quantized version of this model is defined as $f_q(x) = q(w_2)q(w_1)x$, where $q(\cdot)$ is the quantizer from Eq. 1. The quadratic loss for the model is given by

$$\mathcal{L}(f(x)) = \frac{1}{2}\big(w_2 w_1 x - y\big)^2$$

The difference compared to full-precision optimization is then given as

$$\delta_{\mathcal{L}} = \mathcal{L}(f_q(x)) - \mathcal{L}(f(x)) \tag{20}$$

$$= \frac{1}{2}\Big[\big(q(w_2)q(w_1)x - y\big)^2 - \big(w_2 w_1 x - y\big)^2\Big] \tag{21}$$

$$= \frac{1}{2}\Big[\big(q(w_2)q(w_1)x\big)^2 - \big(w_2 w_1 x\big)^2 - 2y\big(q(w_2)q(w_1)x - w_2 w_1 x\big)\Big] \tag{22}$$

$$= \frac{1}{2}x^2\Big[q(w_2)^2 q(w_1)^2 - w_2^2 w_1^2\Big] + yx\Big[w_2 w_1 - q(w_2)q(w_1)\Big] \tag{23}$$

The loss difference decomposes into:

$$\underbrace{\frac{1}{2}x^2\Big(q(w_2)^2 q(w_1)^2 - w_2^2 w_1^2\Big)}_{\text{quadratic term (Oscillator)}} \quad + \quad \underbrace{yx\Big(w_2 w_1 - q(w_2)q(w_1)\Big)}_{\text{linear term (Oscillation Dampener)}} \tag{24}$$

Taking the derivative of $\mathcal{L}$ with respect to w_1:

$$\frac{\partial \delta_{\mathcal{L}}}{\partial w_1} = \frac{\partial}{\partial w_1}\Big(\mathcal{L}(f_q(x)) - \mathcal{L}(f(x))\Big) \tag{25}$$

$$= \frac{\partial}{\partial w_1}\left[\frac{1}{2}x^2\Big(q(w_2)^2 q(w_1)^2 - w_2^2 w_1^2\Big) + yx\Big(w_2 w_1 - q(w_2)q(w_1)\Big)\right] \tag{26}$$

$$= x^2\left[q(w_2)^2 q(w_1)\frac{\partial q(w_1)}{\partial w_1} - w_2^2 w_1\right] + yx\left[w_2 - q(w_2)\frac{\partial q(w_1)}{\partial w_1}\right] \tag{27}$$

Using the STE approximation from Eq. 4, we get:

$$\frac{\partial \hat{\delta}_{\mathcal{L}}}{\partial w_1} = x^2\Big[q(w_2)^2 q(w_1) - w_2^2 w_1\Big] + yx\Big[w_2 - q(w_2)\Big] \tag{28}$$

We note that the linear term is no longer zero in the gradient and thus for a model consisting of 2 single weight layers we see that there is additional effects from QAT other than oscillations. Additionally because of the non-linearity of the rounding operation, even with the absence of a non-linear activation function, we can no longer reduce the model to a single weight.

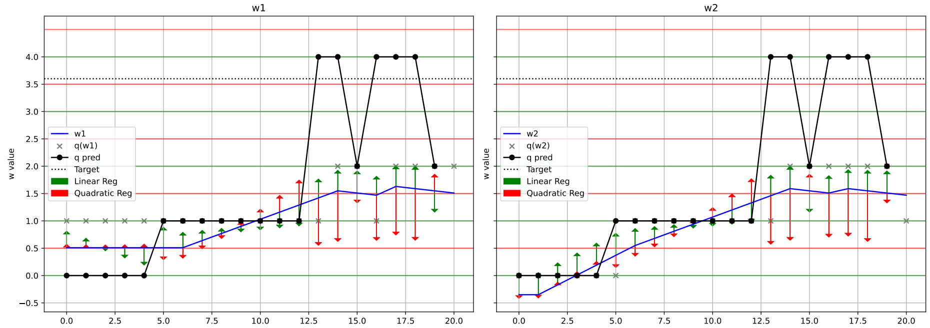

Figure 4: We repeat the toy model experiments, but this time with 2 weights, taking into account that the linear term is no longer 0 in the gradient. We notice at epoch 15 and 18 where the prediction of the quantized model is greater than y, the effect of the terms flip for w_2.

A.2 Hyperparameters

A.2.1 ResNet-18

In Fig. 5 and Fig. 6 we see the results of the λ hyperparameter search over different learning rates for a ResNet-18 model. There is a clear trend of seeing the best performance at a learning rate of 10^{-3}. We note that interestingly there is a comparable performance for a wide range of λs, indicating that it is the presence of oscillations which is important for quantization robustness, and not the exact frequency of oscillations.

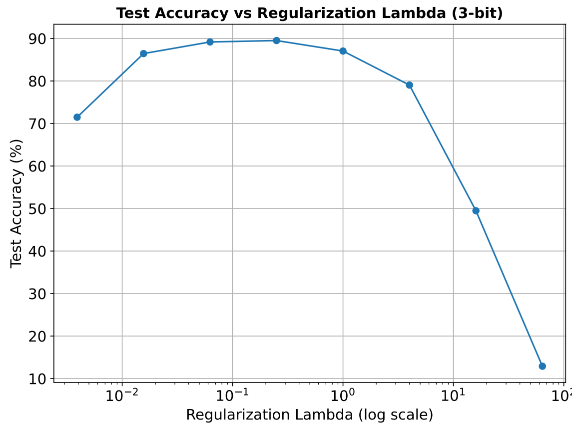

Figure 5: Mean over 3 runs of the best test accuracy for different lambdas. Fine-tuning a pretrained ResNet-18 on CIFAR-10 for 50 epochs. Quantizer is set to 3-bit and 10^{-3} learning rate and 100% of the training data is used.

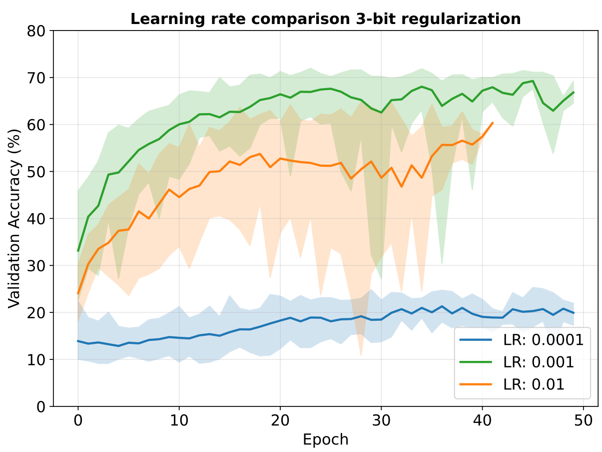

λ	3-bit (%)	Ternary (%)
0.25	68.77 ± 0.19	47.85 ± 5.51
0.50	69.47 ± 1.11	46.77 ± 4.83
0.75	70.08 ± 0.40	46.86 ± 3.01
1.00	66.20 ± 4.05	47.33 ± 2.06
1.25	69.31 ± 0.32	43.14 ± 6.62
1.50	68.96 ± 0.30	46.73 ± 3.91
1.75	69.92 ± 0.11	47.02 ± 4.19

Figure 6: Mean over 3 runs of the best validation accuracy for different lambdas. Training a ResNet-18 from scratch. Both ternary and 3-bit is at 10^{-3} learning rate and 50% of the data used for training. The plot shows three learning rates, where we for each learning ratue evaluate with the λs in the rhs. table. The colored background covers the range between the maximum and minimum value of the quantized validation accuracy with the given λs.

A.2.2 Tiny ViT

Fig. 7 We note how also the Tiny Vit seems to allow for a wide range of λs even though we this time note that $\lambda = 1$ performs significantly better than the others.

A.3 Ternary Quantization

Performance comparison for the ternary quantization for different models and datasets is reported in Table 5. While both QAT and oscillations improve the PTQ baseline significantly, oscillations degrade compared to QAT, especially for the Tiny ViT. This is in line with previous literature (Liu et al., 2023), where transformers

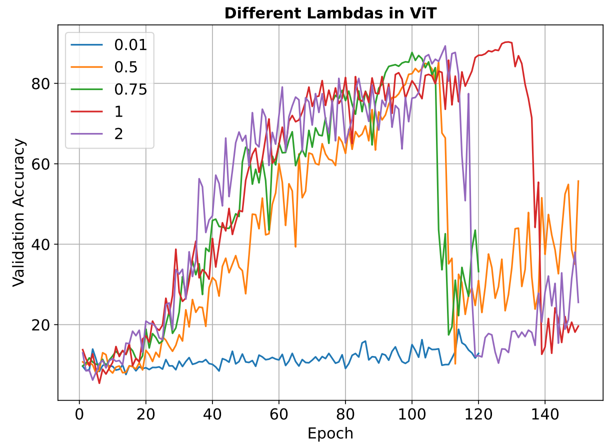

λ	3-bit (%)	Ternary (%)
0.01	18.85	-
0.5	85.21	15.10
0.75	87.68	-
1.0	90.29	13.04
2.0	89.31	14.16
2.5	-	13.70
5.0	-	14.20

Figure 7: Validation accuracy at different λ values and the corresponding best validation accuracies for 3-bit and 2-bit configurations for a single run. Learning rate is set to 1e-4 for fine-tuning. For the 2-bit we test higher λ but still see no improvemenet in accuracy. We note how all the λs lies close to each other, except for the low of 10^{-2}

have been identified as especially sensitive to oscillations. But if oscillations are fundamental to QAT, why does QAT still deliver better ternary performance? In appendix A.1 we are given a clue. Looking at the gradient of the two-layer toy model, in Eq.24 we note that the second term is no longer zero in the gradient. This term bears close resemblance to existing formulations of oscillation dampeners, such as in Eq. 6 (Nagel et al., 2022). These works by pushing weights towards their nearest quantization level, thereby dampening or nullifying the effect of any oscillator (Which pushes weights towards their nearest threshold). We therefore speculate that the main component of QAT is still oscillations, but that QAT also has an inherent dampening mechanism. Given that in a uniform quantizer, the quantization error increases exponentially as we decrease the bits in the quantizer, ternary quantization's large error magnitude makes the absence of dampening particularly detrimental, resulting in sub-optimal quantized performance compared to QAT.

Quantization	MLP5 (FS)	ResNet-18 (FS)	ResNet-18 (FT)	Tiny ViT (FT)
Baseline FP32	51.43 ± 0.39	83.26 ± 1.07	83.26 ± 1.07	96.11 ± 0.31
Ternary PTQ	10.00 ± 0.02	10.00 ± 0.01	10.00 ± 0.01	9.39 ± 1.11
Ternary QAT	49.20 ± 1.34	79.62 ± 6.42	77.02 ± 7.57	73.53 ± 0.77
Ternary Oscillations	36.49 ± 0.51	61.50 ± 1.82	44.59 ± 3.30	13.51 ± 1.32

Table 5: Performance comparison with ternary quantization on CIFAR-10 dataset. Mean and standard deviation is over 3 runs. The models is fine-tuned for 50 epochs on the pretrained ImageNet models. PTQ results is from the FP32 baseline. For both oscillations only and QAT we see a significant improvement over the PTQ baseline. Yet oscillations degrade significantly compared to QAT, especially for the Tiny Vit. FS: Train from scratch. FT: Fine-tuned.

A.4 Cross-bit accuracy

Results with standard deviations over three runs for the cross-bit evaluations are reported in Table 7.

A.5 Epochs and cross-bit robustness

There is an interesting interaction between number of epochs trained and robustness both of our method and QAT. We note how QAT converges first for the target-bit and then over time also converges for the 4 and 8-bit. Additionally we see that QAT seems upper-bounded by the target-bit performance, while this is not the case for oscillations only as shown in Fig. 8.

Model	Method ↓ / Eval. bit →	FP32	Tern.	3-bit	4-bit	8-bit
ResNet-18 (FT)	Baseline PTQ	88.50	10.01	10.28	35.56	88.45
	Ternary QAT	10.39	**77.02**	9.75	10.03	10.35
	Ternary Oscillations	**87.44**	44.59	**85.42**	**87.03**	**87.42**
Tiny ViT (FT)	Baseline PTQ	96.11	9.39	11.56	21.57	96.03
	Ternary QAT	10.62	**73.53**	11.52	11.13	10.61
	Ternary Oscillations	**95.79**	13.51	12.53	**54.93**	**95.76**

Table 6: Cross-bit evaluation of pre-trained ImageNet-1k models fine-tuned on CIFAR-10. Grey background is the target-bit accuracy. Models are trained using different quantization methods (QAT and ours) and bit-widths (ternary, 3-bit, and 4-bit), then evaluated across various bit-widths ranging from ternary to FP32. The grey diagonal shows the results for the bit used during training. Results are means and standard deviations over 5 random seeds. All significant differences between QAT and Oscillations are shown in bold face.

Model	Train bit ↓ / Eval. bit →	FP32	Ternary	3-bit	4-bit	8-bit
ResNet-18	Baseline (PTQ)	88.50 ± 0.64	10.01 ± 0.01	10.28 ± 0.48	35.56 ± 9.05	88.45 ± 0.64
	Ternary QAT	10.39 ± 0.71	**77.02 ± 7.57**	9.75 ± 0.77	10.03 ± 0.51	10.35 ± 0.63
	Ternary Oscillations	**87.44 ± 0.56**	44.59 ± 3.30	**85.42 ± 1.13**	**87.03 ± 0.65**	**87.42 ± 0.56**
	3-bit QAT	16.89 ± 4.97	10.01 ± 0.04	85.69 ± 1.83	17.42 ± 4.96	16.56 ± 4.32
	3-bit Oscillations	**87.86 ± 0.42**	**20.19 ± 10.74**	84.94 ± 1.59	**87.56 ± 0.38**	**87.86 ± 0.42**
	4-bit QAT	87.75 ± 1.13	10.13 ± 0.29	82.08 ± 6.25	87.71 ± 1.14	87.76 ± 1.12
	4-bit Oscillations	87.85 ± 0.49	11.91 ± 0.87	85.57 ± 1.10	87.08 ± 0.72	87.87 ± 0.49
Tiny ViT	Baseline (PTQ)	96.11 ± 0.31	9.39 ± 1.11	11.56 ± 1.99	21.57 ± 5.33	96.03 ± 0.34
	Ternary QAT	10.62 ± 1.29	**73.53 ± 0.77**	11.52 ± 1.82	11.13 ± 1.75	10.61 ± 1.26
	Ternary Oscillations	**95.79 ± 0.58**	13.51 ± 1.32	12.53 ± 3.66	**54.93 ± 27.32**	**95.76 ± 0.59**
	3-bit QAT	86.94 ± 0.91	**19.78 ± 6.04**	88.13 ± 0.60	86.69 ± 0.62	86.95 ± 0.89
	3-bit Oscillations	**96.47 ± 0.11**	9.48 ± 1.64	88.68 ± 1.08	**95.35 ± 0.18**	**96.50 ± 0.11**
	4-bit QAT	95.14 ± 0.29	11.11 ± 1.84	59.86 ± 19.95	94.96 ± 0.33	95.13 ± 0.28
	4-bit Oscillations	**96.54 ± 0.09**	11.90 ± 1.29	70.23 ± 12.75	94.82 ± 0.51	**96.55 ± 0.09**

Table 7: Cross-bit evaluation of pre-trained ImageNet-1k models fine-tuned on CIFAR-10. Grey background is the target-bit accuracy. Models are trained using different quantization methods (QAT and ours) and bit-widths (ternary, 3-bit, and 4-bit), then evaluated across various bit-widths ranging from ternary to FP32. The grey diagonal shows the results for the bit used during training. Results are means and standard deviations over 5 random seeds. All significant differences between QAT and Oscillations are shown in bold face.

A.6 Convergence behaviour during oscillations-only optimization

Fig. 9 shows the convergence behaviour of the full precision weights and the quantized weights at target-bit. We note how the Tiny ViT displays a peculiar convergence behaviour, where the accuracy will break, only to go up again. In the Tiny Vit model we quantize the self-attention layers, it is already noted in Liu et al. (2023) that ViTs are especially vulnerable to quantization of the query and key of a self-attention layer, which might be related to the convergence behaviour we see.

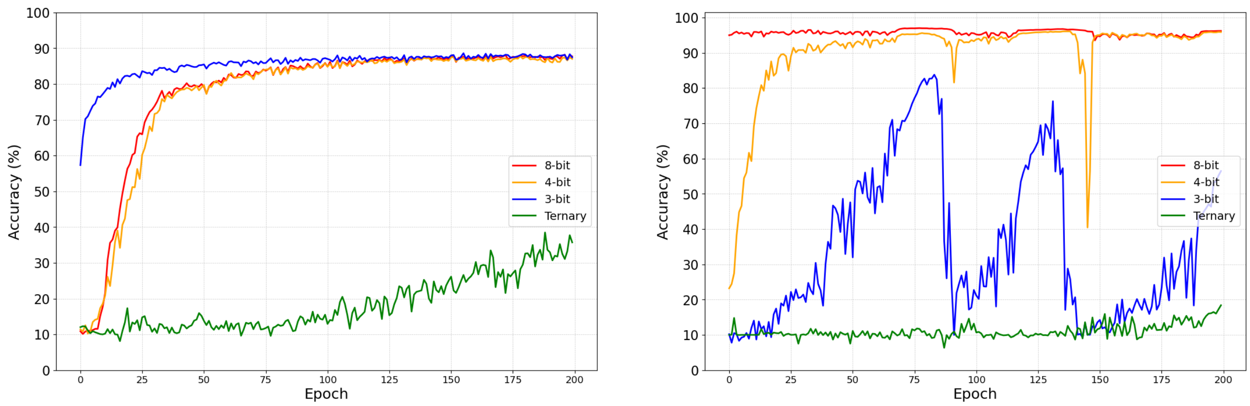

Figure 8: Left is the validation accuracy during training of a ViT with QAT at different bits, right is for our regularization. Both QAT and regularization is trained with a 3-bit quantizer. We note how the order of convergences for cross-bit changes between QAT and our model and that QAT cross-bit robustness especially depends on number of epochs trained.

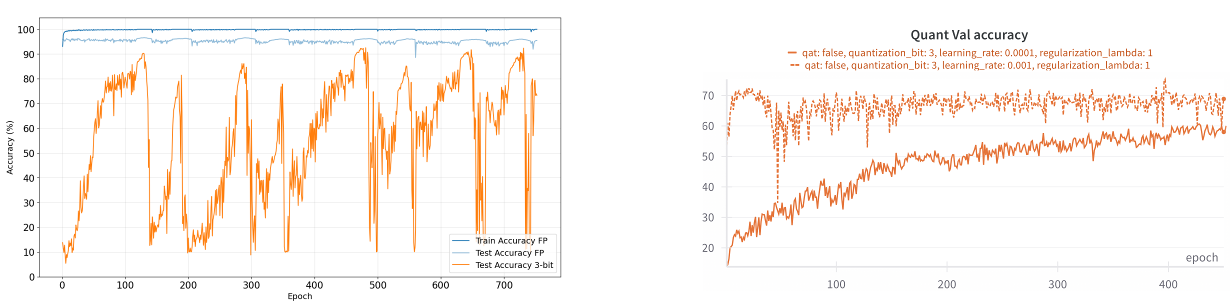

Figure 9: In the right plot we see the convergence behaviour of ResNet-18. In the left plot we see the convergence behaviour of a Tiny ViT with regularization with a 3-bit quantizer. We note the peculiar behaviour of the orange line, which is the validation accuracy on the target-bit performance. The performances cycles between $\approx 90\%$ and 10%, while the full precision accuracy (The model evaluated without quantized weights) stays some-what stable.